Original article

Material and moisture balance in a full-scale bio-drying MBT system for solid recovered fuel production

Geun-Yong Ham[1], Toshihiko Matsuto[1*], Yasumasa Tojo[1], Takayuki Matsuo[1]

[1] *Laboratory of Solid Waste Disposal Engineering, Faculty of Engineering, Hokkaido University, Kita 13, Nishi 8, Kita-ku, Sapporo, Hokkaido 060-8628, Japan*

Geun-Yong Ham: gyham127@gmail.com
Yasumasa Tojo: tojo@eng.hokudai.ac.jp
Takayuki Matsuto: takayuki@eng.hokudai.ac.jp

* Corresponding author. Tel./fax: +81-11-706-6825

E-mail address: matsuto@eng.hokudai.ac.jp

ABSTRACT

Bio-drying MBT is a type of mechanical biological treatment (MBT) system and reduces moisture content of the MSW to improve the separation of combustible fractions. In this study, a full-scale biocell type bio-drying MBT system was investigated. The mass balance of waste component was estimated by composition and characterization of waste and tonnage data. During separation of biodried outputs, 62 % of plastics and 54 % of paper were recovered as RPF material. Wood was decreased by reduction in particle size and 90 % of biodried wood is returned to next reactor. Changes of mixed fine caused by fine wood particle and the loss of organic matters and 60 % of it were returned. Daily water removal during 17-days of bio-drying was simulated through the model by using the operation data. Among the four operation phases, the longest stabilization phase was expected to main water removal period, but half of water removal was occurred at initial two stages and phase IV for only 6

days in total due to the high waste temperature for sanitization (phase I and II) and high airflow rate for cooling. Decreasing waste temperature at phase III resulted in low water evaporation.

Keywords: Bio-drying MBT, Material balance, Water removal, Material recirculation, Solid recovered fuel recovery

Introduction

Formerly, many European Union (EU) countries relied heavily on landfills for waste treatment and disposal. However, as a substantial amount of municipal solid waste (MSW) containing a high portion of biodegradable waste was disposed of at landfills, management of the resulting leachate and gas emissions caused from the biodegradation of organic matters required long-term care [1]. To cope with this problem, the European Commission established the Landfill Directive (99/31/EC), which required the reduction of biodegradable waste in landfills. In response, mechanical-biological treatment (MBT) systems have been developed to reduce the amount of biodegradable waste sent to landfills [2, 3].

In a typical MBT system, mixed MSW is mechanically separated and then undergoes sequential biological and thermal treatments to stabilize organics and the remaining combustible fraction. The resulting stabilized residue is then sent to a landfill for final disposal. MBT systems also present an opportunity for energy recovery in the form of biogas from anaerobic digestion (AD) or a solid recovered fuel (SRF). SRF production has been preferred as it enables thermal recovery in a variety of end-uses at cement kilns or other co-combustion power plants as an alternative to fossil fuels [4–7]. In order to recover more SRF, bio-drying MBT systems can be applied to improve the separation efficiency of the combustible fraction by reducing the moisture content of MSW at first process.

The reactors used in bio-drying MBT systems can be divided into three types: dynamic reactors, static reactors, and windrows. Dynamic reactors are used in continuous systems with counter flow aeration against the waste movement and consist of an inclined rotary drum that is 2 to 4 m in diameter and a maximum of 45 m long. Typical static reactors are enclosed biocell or biocontainer batch-type reactors. A biocell is an enclosed rectangular reactor that has a volumetric capacity in the range of 100 to 1000 m^3 and is, at maximum, 50 m long. Waste is charged to the reactor by a wheel loader or conveyor belt. A biocontainer is smaller

box reactor with a volume of 20 to 40 m^3 in which waste is loaded from the top of the reactor. A windrow pile system has a pile in a triangular or trapezoidal shape where waste is stacked up to 1.5 or 2.0 m high. In static-type and windrow reactors, forced aeration is accomplished from the bottom. Most full-scale Bio-drying MBT systems in operation are enclosed static-type reactors [2, 3, 8].

Tambone et al. investigated the fuel quality and biogas generation potential of biodried outputs from a windrow pile system by analyzing the heating value, respiration index, and biochemical methane potential (BMP) test [9]. Dębicka et al. analyzed the heating value and respiration index of a biocell that has a 150 m^3 to determine the moisture reduction and fuel qualities [10]. Evangelou et al. monitored the composting process of a 360 m^3 biocell-type bio-drying MBT system for 1.5 years to evaluate organic stabilization and the qualities of the resulting fuel by measuring the dynamic respiration index and heating values [11]. Dziedzic et al. studied a 36 m^3 biocontainer to investigate the fuel qualities and biogas generation potential of biodried outputs [12].

Unlike the above MSW-treatment facilities, Winkler et al. studied a 1900 m^3 biocell-type reactor used to treat sewage sludge [13]. In this system, air was recirculated and biodried sludge was returned as a bulking agent and an inoculum. They evaluated the water removal of sewage sludge and estimated the evaporation during the bio-drying process by using the operation data.

In this study, an operating 900 m^3 biocell-type bio-drying reactor employing material and air recirculation was investigated. The produced fuel is recovered after 17 days of the bio-drying process, at which point wood and fine residue are returned to the next reactor. Air in the reactor is recirculated to the reactor by changing the fresh air intake ratio.

Unlike prior studies, this work focuses on the material balance and model estimation of water removal. The material balance of changes during the bio-drying process and during the

separation of biodried materials is estimated by analyzing samples in terms of proximate analysis, total organic carbon (TOC) content, and BMP. Water removal is estimated by analyzing the monitored operation data.

Materials and Methods

Investigation of bio-drying MBT system

Fig. 1 Description of the investigated bio-drying MBT system: (a) process flow and annual mass in the facility and sampling location and (b) schematic diagram of airflow in the reactor

A process flow diagram of the investigated bio-drying MBT system is shown in Fig. 1a. Six biocell reactors (BR) are installed and operated in turn. Each BR has a capacity of 900 m^3, 6 m wide, 5 m high, and 30 m long. After 17 days of bio-drying operation, biodried output is separated into three fractions: raw material for refuse-derived paper and plastics densified fuel (RPF), wood residue and fine residue. Residues are transferred to next BR as bulking agent and inoculation. They are mixed with shredded MSW by a shear shredder (Ø 460 mm) and new wood occasionally, then transferred by a wheel loader to the BR. Water (11.5 to 20.7 m^3) is added to the waste during the first stage of the bio-drying process to promote the biodegradation with mixing generated leachate. Approximately 260 tons of input mixture is processed in one BR. The biodried waste is sorted into heavy, light, and fine matters by a ballistic separator, which is tilted 20 degrees and has screened moving paddles. The heavy and light fractions are separated by gravity with upward airflow. Any inert materials or PVC are removed using an NIR separator.

In October 2018, a total of 30 kg of waste samples were collected from five different locations in the facility, indicated with an S in Fig. 1a. All samples except for the BR input

was taken from one of the BRs after 17 days of operation. BR output, wood residue, and fine residue samples were taken from each pile, and RPF material samples were taken from bailed products. The BR input sample was collected from next BR that was in the filling stage before the process initiation. Residues contained in BR input sample were the outputs of previous BR. MSW and wood were not sampled because MSW was mixed with return residues just after shredding, and wood was hard to collect representative sample due to large size.

The tonnage shown in Fig. 1a indicates the total mount from April 2017 to March 2018. Waste mass was measured either by truck scale (TS) or weighing scale on the wheel loader (LD). Water added to the BR was measured through a flowmeter (FM). The input and output mass of each BR were estimated from the summation of each waste stream.

The overall airflow through the reactor is shown in Fig. 1b, in which the mixture of fresh air and recirculating air from the BR is used for aeration of the waste. During the process, the airflow rate and mixing ratio of fresh air is controlled according to the waste temperature. The details of the control mode and variables shown in the figure are explained in final section.

Laboratory analyses and procedures

To determine moisture content, the collected samples were dried in a drying oven (hot-air circular drying machine, Toyo) at 50 °C until the changes of sample weight showed below 1% variance. Samples were manually turned two times a day. Moisture content was determined by the difference of weight for each sample. Dried samples were hand-sorted into six components: plastics, paper, textiles, wood, incombustibles, and mixed material. Mixed material was then sieved with a 4.0 mm screen, at which point the oversized fraction was sorted into its components and undersized fraction was categorized as mixed fine.

For further analysis, samples were ground by cutting mill (MRK-Retsch Ultra cutting mill, Country). As this mill could not grind textiles, they were cut into small pieces using scissors and then ground with a freeze grinder (AS One Freeze grinder, TPH-02). All samples were analyzed for combustible and TOC content. A BMP test was conducted to determine biogas generation as an index of biodegradable organics.

To measure the combustible contents, 5 g of each dried sample were placed in a crucible and ignited using a muffle furnace (Box furnace KBF-894N1) at 800 °C for 2 hours. The TOC content was determined by the difference between the total carbon (TC) and inorganic carbon (IC) of 30 mg dried samples using a TOC-TN analyzer (TOC-V CPH/CPN, connected with TOC-V SSM-5000A Shimadzu Corporation). Pure glucose ($C_6H_{12}O_6$) and sodium carbonate (Na_2CO_3) were used as a standard carbon source for the TC and IC analysis, respectively.

The BMP was experimentally analyzed as done by Hansen et al. and Pantini et al. [14, 15]. Here, one gram of the sample was mixed with 40 mL of distilled water and 20 mL of inoculum in a 135 mL vial. The samples were then purged with nitrogen to remove traces of oxygen and sealed with a butyl rubber stopper and aluminum crimps. The test materials were incubated at 55 °C for 28 days; paper and textiles were incubated for 35 days due to prolonged biodegradation. The inoculum used was taken from the liquid sludge of an AD process at Fuji Clean Center in Kagawa, Japan.

Generated biogas was extracted by inserting a 50 or 100 mL syringe until the piston movement stopped, at which point the gas volume generated was measured. Then, 0.1 mL of gas was withdrawn using a 0.5 mL gas syringe; the gas composition was determined by gas chromatography (GC-TCD, HITACHI, type 164). Gas was extracted every day during the initial stage and every 2–3 days afterwards. Gas generation was adjusted by subtracting the

amount found in a blank containing only water and sludge. After 28 or 35 days (depending on the material) of testing, the gas composition of the air phase of the vial was also measured.

Results and Discussion

Physical composition and waste characterization

Fig. 2 Physical composition of waste on a wet basis

The physical composition of the five samples taken from the facility is shown on a wet basis in Fig. 2. From the input to the output, the moisture content decreased from 40% to 28 % from BR and rest were shown around 20 % or less. In the wood and fine residue, a considerable amount of wood and mixed fine material was contained. Because MSW and wood were not available for sampling as mentioned in above, the composition of MSW and new wood was assumed based on the literature values. The data of MSW was referred to the report of incineration facility in Mitoyo city [16]. High moisture content of MSW is caused by 61 % of food wastes. Large sized hard wood is introduced to keep porosity [17].

Fig. 3 Waste characteristics of (a) combustible content and (b) gasified carbon in biogas

The determined TOC content, combustible content, and gasified carbon in biogas through BMP test are compared in Fig. 3, where each component is plotted using same symbols, but BR input samples are differentiated by no colored mark, as they contained fresh MSW. The

147 striped mark in each component indicates the characteristics of MSW and new wood as
148 reference [17, 18]. Food wastes that only exist in MSW were marked by star mark.

149 In Fig. 3a, the TOC/combustibles indicate the characteristics of the combustible fraction,
150 where a low combustibility was caused by contaminated inorganic materials. The broken
151 lines in Fig. 3a represent the characteristics of polyethylene and cellulose [17]. The
152 TOC/combustibles of plastics is similar to polyethylene. The TOC/combustibles of textiles
153 that is slightly higher than cellulose suggests that they are composed of synthetic and natural
154 fibers. The TOC/combustibles of the mixed fine component was similar to that the textile
155 component, suggesting that it contained high-carbon-content organics, such as humic
156 substances. Referred characteristics of MSW and new wood are similar to the sample analysis
157 results.

158 The gasified carbon by anaerobic digestion, or gasified carbon in the biogas, determined by
159 the BMP test and TOC content of waste components are compared in Fig. 3b. The ratio of
160 gasified carbon to TOC is 60% for paper, 5%–10% for wood and plastics, and 30% for
161 textiles and mixed fine components. The generated gas from plastics was caused by attached
162 organic material. The determined biogas generation of textiles is reasonable, considering they
163 likely consisted of synthetic and natural fibers. The low ratio of gasified carbon to TOC in the
164 mixed fine components is reasonable, as they consist of stabilized and/or hardly
165 biodegradable organics output from the BR.

166 Comparing each component in Fig. 3a and 3b, no significant differences were seen among
167 the samples, even between the input to and output of the BR. This is likely because the partial
168 reduction of organic matters after the 17-day bio-drying process is only the decrease of the
169 amount and its characteristics including BMP test was not changed.

170

171 **Component mass fraction by waste stream**

Fig. 4 Mass fraction of (a) dry solids, (b) gasified carbon in biogas, and (c) combustibles of each waste stream component on a dry basis, normalized by the total dry mass of the INPUT

Fig. 4 was obtained by multiplying the mass in Fig. 1 with the physical composition in Fig. 2 for each waste stream in dry basis excluding moisture. As shown by the arrows on the top of the figure, the sum of RPF materials, wood residue and fine residue were output from the BR, and the input to the BR consisted of wood residue, fine residue, MSW, and new wood. Results of sample analysis for BR input and BR output were not used in the calculation as it was considered less creditable than the summation of other samples in terms of the homogeneity.

Fig. 4a was normalized by the total dry mass of the input. In this figure, 76% of wood originates from the return residue, whereas 17% is provided from new wood. For the RPF materials, i.e., plastics and paper, 60% was introduced through the MSW stream, whereas 40% was from returned residue.

Fig. 4b–c were calculated similarly for gasified carbon in biogas and combustibles by multiplying their characteristics (Fig. 3) with the dry mass of each component in Fig. 4a. The mass fraction of combustibles in Fig. 4c looks similar to the dry solids in Fig. 4a.

Separation efficiency of output from BR

Table 1. Separation ratio of the output streams on a dry basis

195 The separation ratio of the output from the BR into the three streams for total dry mass and
196 each waste component was calculated from the data in Fig. 4a and is shown in Table 1.
197 Of the fuel materials, only 62% of plastics and 54 % of paper was recovered as a fuel and
198 the rest were returned to the next BR. To investigate the cause of unrecovered materials, the
199 size distribution for RPF materials and wood residue was measured and is shown in
200 Supplementary material. The unrecovered ratio was approximately 40% and was considered
201 as the performance of wind separation. The size of recovered plastic particles ranged from 5
202 cm to 65 cm. The recovery rate of plastic particles to RPF materials under 15 cm in size was
203 only 28%. However, the paper components were mostly smaller than 20 cm and had a
204 recovery rate to RPF of 54%. Wood and the mixed fine component were separated into return
205 stream more effectively; 90% of the wood and 60% of the mixed fine components were
206 returned to the mixer before being introduced to the next BR.
207
208 **Mass balances before and after the bio-drying process**
209
210 **Fig. 5** Mass balances of (a) dry solids, (b) gasified carbon in biogas, and (c) combustibles in
211 the bio-drying process on a dry basis
212
213 The difference in dry mass of each component between the input and output of the bio-
214 drying process is shown in Fig. 5a, where the mass fraction of each component was
215 calculated by summing up for INPUT and OUTPUT in Fig. 4a, and they are depicted by bar
216 graph and dot, respectively. The food waste included in the MSW was added to the mixed
217 fine component in the process input stream. Fig. 5b–c, for gasified carbon in biogas and
218 combustibles, were calculated from Fig. 4b–c in the same manner.

219 The small reduction of paper shown in Fig. 5a is reasonable, as paper does not fully
220 degrade even during the 6 to 8 weeks of the composting process [19]. As wood is a hardly
221 biodegradable organic, the decrease of wood may have been caused by a reduction in particle
222 size, allowing the fine particles to be transferred to the mixed fine component. The reduction
223 in Fig. 5b can be explained by the transfer of wood, and the loss of organic matters can be
224 another reason. Also, no changes of combustibles of mixed fine in Fig. 5c also proved by
225 same reason.
226 The gasified carbon in biogas was reduced by 13% between the input and output of the
227 bio-drying process (Fig. 5b). Among the waste components in the input, food wastes in the
228 MSW and the mixed fine component could be biodegraded in 17 days of the bio-drying
229 process, and their fractions were 13% and 9% of the input, respectively. A decrease from 21%
230 to 13% can be considered reasonable for biodegradation.
231
232 **Water removal during the bio-drying process**
233 To estimate the water removed during bio-drying, the evaporated water mass was then
234 calculated. As shown in Fig. 1b, the four unknown airflow rates were V_A, V_F, V_{RE}, and V_{EX},
235 where subscripts A, F, RE, and EX refer to aeration, fresh air, recirculating air, and exhaust
236 air, respectively. A mixture of fresh air and recirculating air from the BR is aerated to the
237 same BR. The mass and heat balances before and after the mixing of air can be written as Eq.
238 (1) and (2), respectively.

$$V_A = V_F + V_{RE} \quad (1)$$

$$V_A T_A = V_F T_F + V_{RE} T_{RE} \quad (2)$$

239 The ratio of fresh air to total aeration λ_F can be defined as Eq. (3). The recirculating airflow
240 rate can be then determined as Eq. (4). Equation (5), derived from Eq. (2) by substituting V_F
241 and V_{RE} with Eq. (3) and (4), respectively, can then be used to calculate λ_F.

$$\lambda_F = \frac{V_F}{V_A} \quad (3)$$

$$V_{RE} = (1 - \lambda_F) \times V_A \quad (4)$$

$$T_A(℃) = \lambda_F \times T_F + (1 - \lambda_F) \times T_{RE} \quad (5)$$

In Eq. (5), T_{RE} was assumed equal with waste temperature (T_S). The exhaust airflow rate, V_{EX}, was determined to equal V_F by assuming steady state. The value of T_F was assumed as 22.8 °C with 57.9% relative humidity (RH) based on meteorological data [20]. The total aeration flow rate V_A can then be calculated by Eq. (6) where 16000 is the specified airflow rate of the fan in m^3/h, and q_A is the fan speed as a percentage.

$$V_A\ (m^3/h) = 16000 \times q_A \quad (6)$$

The water removal rate in the BR can then be calculated as the difference between the water inlet through fresh air from water outlet, shown in Eq. (7), where X represents the water vapor per unit volume of air in g/m^3, which is a function of water vapor pressure (pv) and temperature (T) (Eqs. (8)–(10)).

$$Water\ removal\ rate\ (kg/h) = (V_{EX} \times X_{EX} - V_F \times X_F) \times 10^{-3} \quad (7)$$

$$X\ (g/m^3) = \frac{217 \times pv}{273.15 + T} \quad (8)$$

$$pv\ (Pa) = RH \times pvs \quad (9)$$

$$\text{When saturated: } pvs\ (Pa) = 6.1078 \times 10^{\frac{7.5 \times T}{T + 237.3}} \quad (10)$$

As shown in Eq. (7), water removal rate is mostly governed by air flow rate V_{EX} and X_{EX}, which is water vapor per unit volume of air. X_{EX} increases exponentially with temperature by Eq. (8)-(10). So, airflow rate and temperature are two major factors for moisture removal.

Exhaust air was assumed to always be saturated and its temperature (T_{EX}) was equal to the waste temperature (T_S).

Fig. 6 Profiles of (a) operation variables and (b) water removal rate under different operation phase during the bio-drying process

The profiles of operation variables are shown in Fig. 6a. Points of irregular operation were removed from the figure but considered in the calculation. The process was subjected to four consecutive operation phases for 17 days. During warm-up (I), a low airflow rate was used to warm to and then maintain the waste at 70 °C for sanitization purposes (II). During stabilization (III), moisture was removed by increasing the airflow rate. The ratio of fresh air was decreased with the progress of biodegradation, as indicated by lowering waste temperature. During the cooling phase (IV), a maximum airflow rate of fresh air (i.e., $\lambda_F = 1$) was provided.

The daily water removal rate as calculated by Eq. (7) is shown in Fig. 6b, where the numbers on the figure indicate the portion of water removed at each phase over the total water removal. Half of the water removal occurred during phase III, which had the longest elapsed time, and the moisture removal rate declined with the decrease of temperature. Phase I and II showed relatively higher removal rate despite their of short duration and low airflow rate, as the saturated moisture content in air is 198 g/m^3 high at 70 °C while 104 g/m^3 at 55 °C. In phase IV, the water removal rate was lowered due to the decrease in temperature, but the maximum flow rate of fresh air for 3 days enhanced moisture removal.

The estimated total water removed, as shown in Fig. 6b, was 86.6 tons. Based on the material flow in Fig. 1 and the moisture content in Fig. 2, the amount of water removed was 55.5 tons, from 105.3 ton to 49.8 ton for 260 tons of wet waste per BR. The difference may have been caused by metabolic water generation or sampling error.

Conclusions

In this study, a full-scale biocell type bio-drying MBT system was investigated. Mass balance of each waste component was estimated by using composition analysis, characterization of waste samples, and waste tonnage data. During separation of biodried outputs, 62 % of plastics and 54 % of paper were recovered as raw material for RPF. The ratios are not low because unrecovered plastics and paper were returned to next biocell reactor. Due to low biodegradation of plastics and paper for 17-days of bio-drying, almost 100 % of the RPF materials could be recovered. Wood was decreased by reduction in particle size during the bio-drying process, 90 % of wood was returned to next BR. Mixed fine seems barely reduced, but reduced wood particle moved to mixed fine and filled up the loss caused by organic degradation and 60 % of mixed fine was returned to next BR.

Water removal phenomena was simulated by the model of daily water removal by using the operation data. The process was subjected to four distinct operation phases and was operated according to the waste temperature. The main phase of water removal was expected to be occurred in stabilization phase (III) for 11 days. However, half of water removal was occurred at initial two phases and phase IV for only 6 days in total and this is caused by high waste temperature for sanitization (phases I and II) and high airflow rate for cooling phase. Phase III was long, but decreasing temperature resulted in low water evaporation.

The findings of this study which are separation efficiency of biodried outputs and effects of temperature and airflow rate on drying efficiency, can give some contribution on improving the full-scale bio-drying MBT system.

Acknowledgement

The authors would like to thank the Biomass Resource Center Mitoyo for their cooperation with waste sampling and interviews.

References

1. Brennan RB, Healy MG, Morrison L, et al (2016) Management of landfill leachate: The legacy of European Union Directives. Waste Manag 55:355–363. https://doi.org/10.1016/j.wasman.2015.10.010
2. Juniper Consultancy Services Ltd (2005) Mechanical-Biological Treatment: A Guide for Decision Makers, Processes, Policies and Markets
3. Velis CA, Longhurst PJ, Drew GH, et al (2009) Biodrying for mechanical-biological treatment of wastes: A review of process science and engineering. Bioresour Technol 100:2747–2761. https://doi.org/10.1016/j.biortech.2008.12.026
4. Velis CA, Wagland S, Longhurst P, et al (2013) Solid recovered fuel: Materials flow analysis and fuel property development during the mechanical processing of biodried waste. Environ Sci Technol. https://doi.org/10.1021/es3021815
5. Velis CA, Longhurst PJ, Drew GH, et al (2010) Production and quality assurance of solid recovered fuels using mechanical-biological treatment (MBT) of waste: A comprehensive assessment. Crit Rev Environ Sci Technol 40:979–1105. https://doi.org/10.1080/10643380802586980
6. Defra (2007) Mechanical biological treatment for municipal solid waste
7. Montejo C, Tonini D, Márquez M del C, Fruergaard Astrup T (2013) Mechanical-biological treatment: Performance and potentials. An LCA of 8 MBT plants including waste characterization. J Environ Manage 128:661–673. https://doi.org/10.1016/j.jenvman.2013.05.063
8. Chiumenti A, Chiumenti R, Diaz L, et al (2005) Modern Composting Technologies. the JG Press Inc.
9. Tambone F, Scaglia B, Scotti S, Adani F (2011) Effects of biodrying process on municipal solid waste properties. Bioresour Technol 102:7443–7450. https://doi.org/10.1016/j.biortech.2011.05.010

10. Dębicka M, Żygadło M, Latosińska J (2017) The effectiveness of biodrying waste treatment in full scale reactor. Open Chem 15:67–74. https://doi.org/10.1515/chem-2017-0009
11. Evangelou A, Gerassimidou S, Mavrakis N, Komilis D (2016) Monitoring the performances of a real scale municipal solid waste composting and a biodrying facility using respiration activity indices. Environ Monit Assess 188:. https://doi.org/10.1007/s10661-016-5303-6
12. Dziedzic K, Łapczynska-Kordon B, Malinowski M, et al (2015) Impact of aerobic biostabilisation and biodrying process of municipal solid waste on minimisation of waste deposited in landfills. Chem Process Eng - Inz Chem i Proces 36:381–394. https://doi.org/10.1515/cpe-2015-027
13. Winkler MKH, Bennenbroek MH, Horstink FH, et al (2013) The biodrying concept: An innovative technology creating energy from sewage sludge. Bioresour Technol 147:124–129. https://doi.org/10.1016/j.biortech.2013.07.138
14. Hansen TL, Schmidt JE, Angelidaki I, et al (2004) Method for determination of methane potentials of solid organic waste. Waste Manag 24:393–400. https://doi.org/10.1016/J.WASMAN.2003.09.009
15. Pantini S, Verginelli I, Lombardi F, et al (2015) Assessment of biogas production from MBT waste under different operating conditions. Waste Manag 43:37–49. https://doi.org/10.1016/J.WASMAN.2015.06.019
16. Mitoyo city (2015) Solid Waste Management Master Plan for Mitoyo city. Mitoyo city, Kagawa, Japan
17. Tchobanoglous G, Theisen H, Vigil SA (1993) Integrated solid waste management : engineering principles and management issues. McGraw-Hill
18. Bae SJ (2005) Estimation of ultimate methane yields from municipal solid waste

components using BMP test. University of Seoul, Korea

19. Alvarez JVL, Larrucea MA, Bermúdez PA, Chicote BL (2009) Biodegradation of paper waste under controlled composting conditions. Waste Manag 29:1514–1519. https://doi.org/10.1016/J.WASMAN.2008.11.025

20. Japan Meteorological Agency (2019) Past weather by city. https://www.data.jma.go.jp/risk/obsdl/index.php#!table

Figure captions:

Fig. 1 Description of the investigated bio-drying MBT system: (a) process flow and annual mass in the facility and sampling location and (b) schematic diagram of airflow in the reactor

Fig. 1a - S mark, collected waste samples; TS, truck scale; FM, flow meter; LD, weighing scale on the wheel loader; SUM, Mass sum of each waste stream

Fig. 1b – Symbols: V, airflow rate; T, temperature; D, degree of openness in damper; q, fan speed in percentage unit

Subscript: F, fresh air; A, total aeration; S, solid waste; EX, exhaust air; RE, recirculating air

Variables in box are given data by the bio-drying process monitoring

(These figures show the details of the investigated bio-drying MBT system.)

Fig. 2 Physical composition of waste on a wet basis

Misc. comb.: Miscellaneous combustibles

(This figure shows the physical composition of the collected waste sample and referred MSW and new wood)

Fig. 3 Waste characteristics of (a) combustible content and (b) gasified carbon in biogas

No colored marks indicate 'BR input' samples which includes fresh MSW; Colored marks indicate 'BR output' and other separated waste stream; Striped marks indicate referred characteristics of MSW and new wood

DS: Dry solids

(These figures show the results of sample analysis for its combustible fraction and biological degradable organics indicated by gasified carbon amount in biogas)

Fig. 4 Mass fraction of (a) dry solids, (b) gasified carbon in biogas, and (c) combustibles of each waste stream component on a dry basis, normalized by the total dry mass of the INPUT

Misc. comb.: Miscellaneous combustibles

389 (These figures show the weighted mass fraction of dry solids, gasified carbon in biogas and
390 combustibles by each composition in different waste stream on a dry basis. Mass fraction was
391 normalized by the total dry mass of the INPUT.)

392 **Fig. 5** Mass balances of (a) dry solids, (b) gasified carbon in biogas, and (c) combustibles in
393 the bio-drying process on a dry basis

394 (These figures show the mass balance of the bio-drying process in terms of the total dry
395 solids, gasified carbon in biogas and combustibles)

396 **Fig. 6** Profiles of (a) operation variables and (b) water removal rate under different operation
397 phase during the bio-drying process

398 I: Warm-up phase; II: Sanitization phase; III: Stabilization phase; IV: Cooling phase

399 T_S, waste temperature; V_A, flow rate of total aeration; V_F, flow rate of fresh air

400 Numbers in Fig. 6b indicate the water removal portion

401 (These figures show the profiles of operation variables and daily water removal rate under
402 different phase during the bio-drying process.)

403

Table 1. Separation ratio of 'OUTPUT' streams in dry basis

		RPF materials	Wood residue	Fine residue
Total dry mass		0.39	0.42	0.19
Material	Plastics	0.62	0.31	0.07
	Paper	0.54	0.30	0.16
	Textiles	0.68	0.25	0.06
	Wood	0.06	0.90	0.04
	Mixed fine	0.33	0.08	0.60

Fig. 1 Description of the investigated bio-drying MBT system: (a) process flow and annual mass in the facility and sampling location and (b) schematic diagram of airflow in the reactor

Fig. 1a - S mark, collected waste samples; TS, truck scale; FM, flow meter; LD, weighing scale on the wheel loader; SUM, Mass sum of each waste stream

Fig. 1b – Symbols: V, airflow rate; T, temperature; D, degree of openness in damper; q, fan speed in percentage unit

Subscript: F, fresh air; A, total aeration; S, solid waste; EX, exhaust air; RE, recirculating air

Variables in box are given data by the bio-drying process monitoring

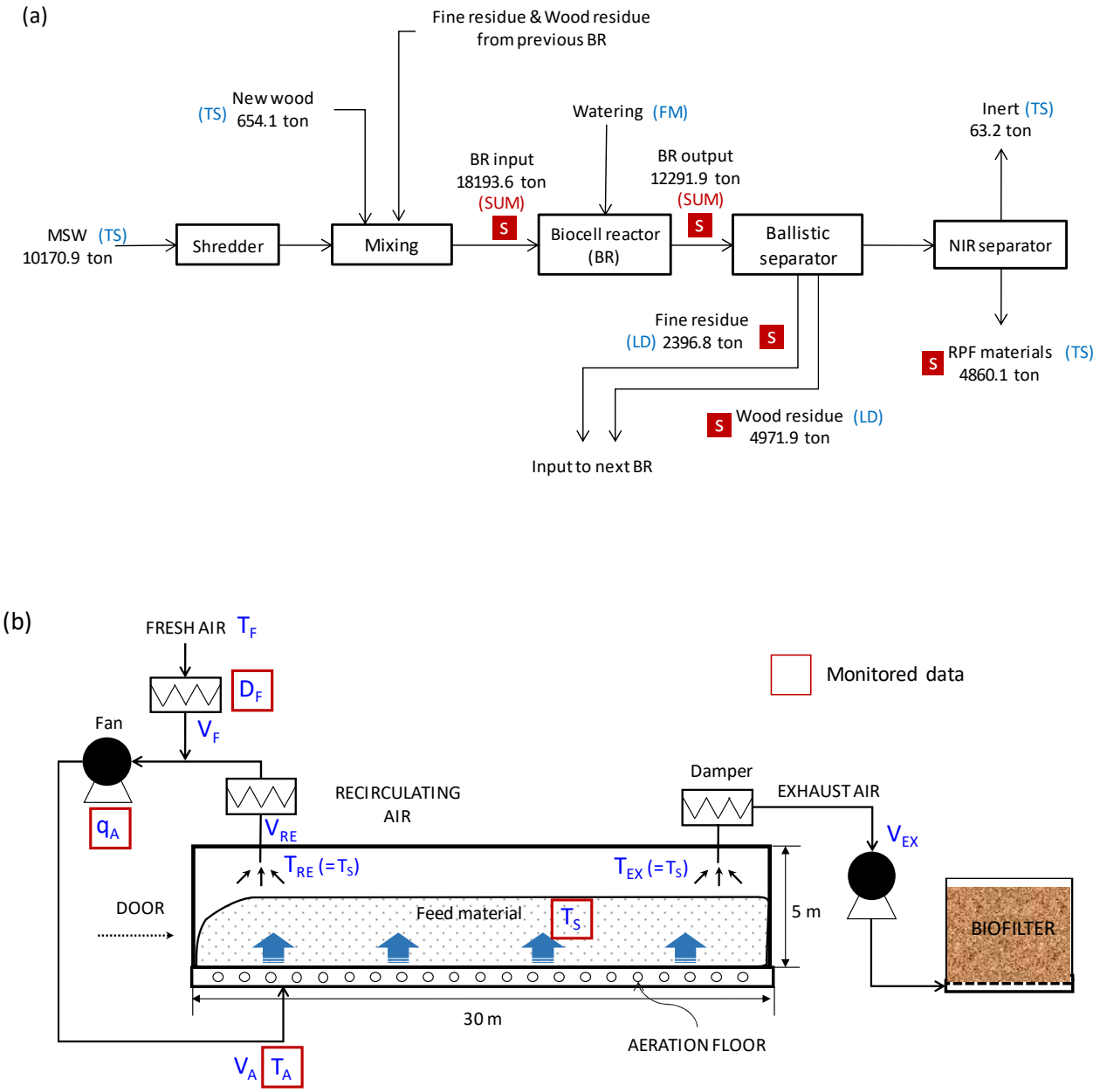

Fig. 2 Physical composition of waste on a wet basis

Misc. comb.: Miscellaneous combustibles

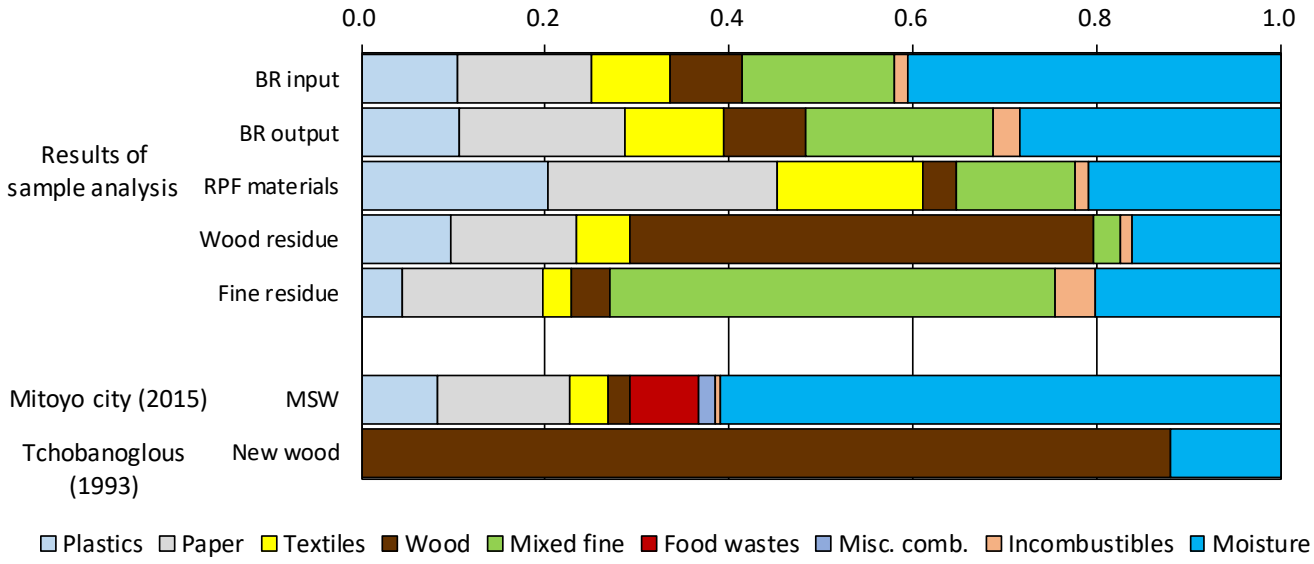

Fig. 3 Waste characteristics of (a) combustible content and (b) gasified carbon in biogas

No colored marks indicate 'BR input' samples which includes fresh MSW; Colored marks indicate 'BR output' and other separated waste stream; Striped marks indicate referred characteristics of MSW and new wood

DS: Dry solids

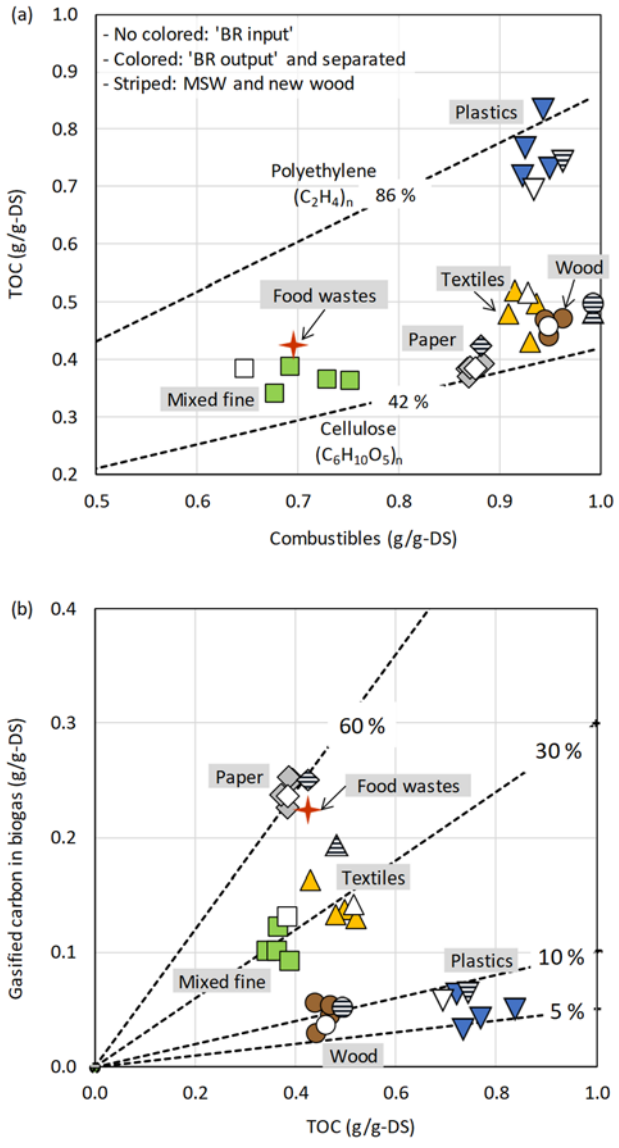

Fig. 4 Mass fraction of (a) dry solids, (b) gasified carbon in biogas, and (c) combustibles of each waste stream component on a dry basis, normalized by the total dry mass of the INPUT

Misc. comb.: Miscellaneous combustibles

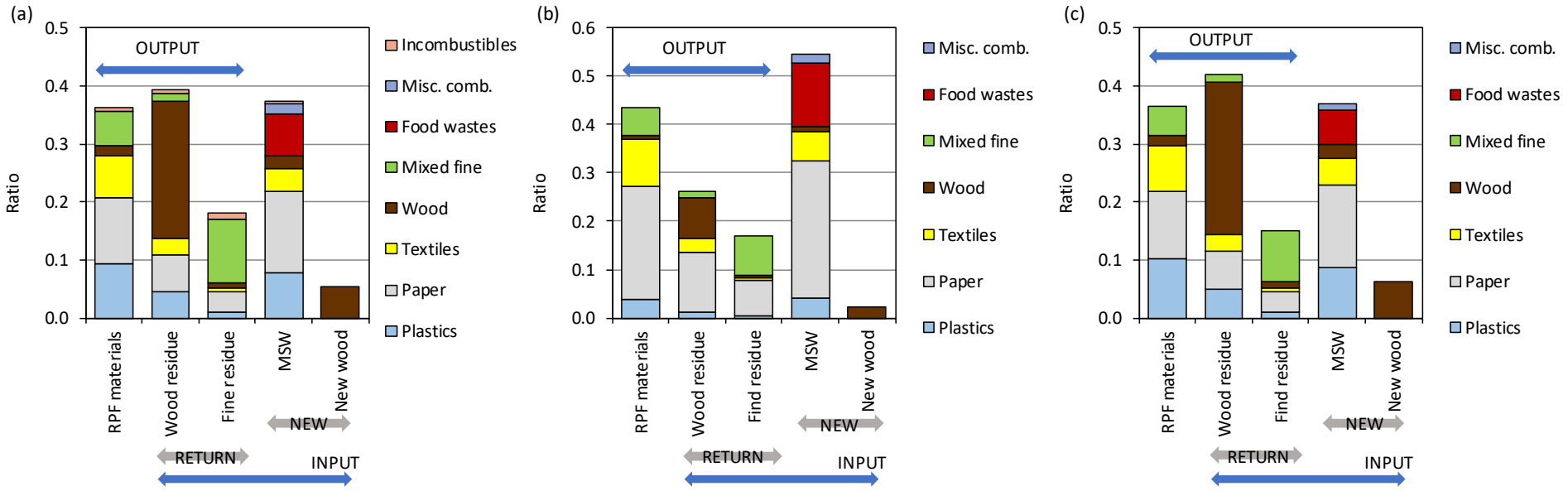

Fig. 5 Mass balances of (a) dry solids, (b) gasified carbon in biogas, and (c) combustibles in the bio-drying process on a dry basis

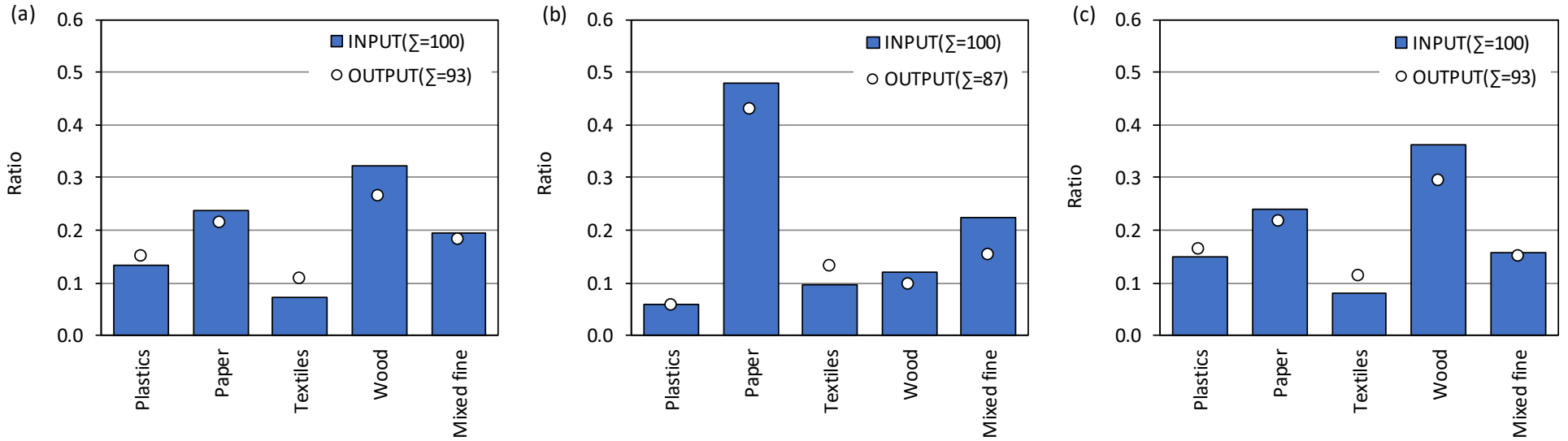

Fig. 6 Profiles of (a) operation variables and (b) daily water removal rate under different operation phase during the bio-drying process

I: Warm-up phase; II: Sanitization phase; III: Stabilization phase; IV: Cooling phase

T_S, waste temperature; V_A, flow rate of total aeration; V_F, flow rate of fresh air

Numbers in Fig. 6b indicate the water removal portion